Multifractal characterization for bivariate data

R. Leonarduzzi, P. Abry, S. Roux
Univ Lyon, Ens de Lyon, Univ Claude Bernard,
CNRS, Laboratoire de Physique, Lyon, France.
roberto.leonarduzzi@ens-lyon.fr

H. Wendt
IRIT, Univ. Toulouse,
CNRS, Toulouse, France.
herwig.wendt@irit.fr

S. Jaffard, S. Seuret
LAMA, Univ. Paris-Est,
UPEM, UPEC, CNRS, Créteil, France.
stephane.jaffard@u-pec.fr

***Abstract*—Multifractal analysis is a reference tool for the analysis of data based on local regularity, which has been proven useful in an increasing number of applications. However, in its current formulation, it remains a fundamentally univariate tool, while being confronted with multivariate data in an increasing number of applications. Recent contributions have explored a first multivariate theoretical grounding for multifractal analysis and shown that it can be effective in capturing and quantifying transient higher-order dependence beyond correlation. Building on these first fundamental contributions, this work proposes and studies the use of a quadratic model for the joint multifractal spectrum of bivariate time series. We obtain expressions for the Pearson correlation in terms of the random walk and a multifractal cascade dependence parameters under this model, provide complete expressions for the multifractal parameters and propose a transformation of these parameters into natural coordinates that allows to effectively summarize the information they convey. Finally, we propose estimators for these parameters and assess their statistical performance through numerical simulations. The results indicate that the bivariate multifractal parameter estimates are accurate and effective in quantifying non-linear, higher-order dependencies between time series.**

I. Introduction

Context: Multifractal analysis. Multifractal analysis is a signal processing tool that provides a robust characterization of data in terms of pointwise regularity properties [1], [2]. It does so through an upper-bound $\mathcal{L}$ for the so-called multifractal spectrum, which quantifies geometrically the pointwise regularity fluctuations of data. Such fluctuations produce, on average, scale-free dynamics, and are thus efficiently modeled and analyzed through the paradigm of scale-invariance. Multifractal analysis has led to significant successes in many real-world applications in very different contexts [3]–[8], and is nowadays established as a versatile and standard signal processing tool. However, it remains essentially univariate, which constitutes a major limitation in view of the increasing number of applications involving multivariate data in many domains. Indeed, multifractal analysis is currently conducted independently for each component in such cases, hence not accounting for the joint information and cross-dependencies in the data. Surprisingly, attempts to extend it to a multivariate setting remain scarce (see, e.g., [9], [10] for notable exceptions in specific applicative contexts).

Related works. State-of-the-art tools for multifractal analysis rely on the use of wavelet leaders, defined through a nonlinear transformation of wavelet coefficients (see Section II-B, and also [11] for a discussion and references on alternative formalisms). Very recently, the first cornerstone for a theoretical foundation of multivariate multifractal analysis was laid in [12] (see also [9] for the first historical work on the topic, in the context of turbulence). Moreover, in the recent contribution [13] a bivariate multifractal random process was defined and studied, following earlier work in [14]. Further, [13] defined a bivariate wavelet leader multifractal formalism and studied it numerically, yielding first intuitions on what type of information is actually captured by the bivariate multifractal spectrum and showing that multifractal features can effectively capture transient, local dependencies that cannot be accounted for by the Pearson correlation coefficient.

Goals, contributions and outline. The present contribution aims to build on, complement and go beyond [13] in several ways. First, in Section II-C the analysis of [13] of the bivariate multifractal spectrum is refined, a quadratic (i.e., second order) model for the bivariate multifractal spectrum is proposed, and the exact expression for $\mathcal{L}$ under this model is obtained. Second, in Section II-D, a parametrization of $\mathcal{L}$ in natural coordinates is derived, effectively capturing the leading-order information contained in the multifractal spectrum in a small number of easily interpretable quantities. Third, Section III-C derives an expression for the Pearson correlation coefficient of the model introduced in [13], [14], which complements the analysis in [13] and provides a natural expansion of the joint dependence structure of the quadratic multifractal model in an (additive) self-similar random walk correlation and a (multiplicative) multifractal correlation. Finally, Section IV studies the performance of the estimators proposed for all parameters of the model through Monte Carlo simulations using synthetic multifractal data.

II. Bivariate multifractal analysis

A. Multifractal spectrum

The goal of multifractal analysis is the quantification of the fluctuations along time of the regularity of a signal or function $X(t)$ at position $t \in \mathbb{R}$, see, e.g., [1]. Pointwise regularity is usually measured using the Hölder exponent, $h(t) \geq 0$, as follows: X is said to be in $C^\alpha(t)$, $\alpha \geq 0$, if there exist a polynomial P_t with $\deg(P_t) < \alpha$ and a constant $C > 0$ such that

$$|X(t+a) - P_t(t+a)| \leq C|a|^\alpha, \ |a| \to 0, \tag{1}$$

$h(t)$ is defined as the largest α such that (1) is satisfied,

$$h(t) \triangleq \sup\{\alpha : X \in C^\alpha(t)\} \geq 0. \tag{2}$$

ISBN 978-90-827970-1-5

The closer $h(t)$ to 0, the more irregular X is around t.

Let $\mathbf{h}(t) \triangleq (h_1(t), h_2(t))$ denote the Hölder exponents of the components of the bivariate signal $\mathbf{X} = (X_1, X_2)$. The *bivariate multifractal spectrum* $\mathcal{D}(h_1, h_2)$ of X is defined as the collection of Hausdorff dimensions $\dim_H$ of the sets of points $t \in \mathbb{R}$ at which $(h_1(t), h_2(t))$ takes on the values $\mathbf{h} = (h_1, h_2)$ [9], [12],

$$\mathcal{D}(h_1, h_2) \triangleq \dim_H \big\{ t : (h_1(t), h_2(t)) = (h_1, h_2) \big\}. \quad (3)$$

It provides a global, geometrical description of the pointwise regularity properties of the components of X. Its precise shape and width, and its orientation with respect to the h_1, h_2 axes, quantify information regarding the joint local fluctuation and dependence of the regularity of the components of X.

B. Wavelet leader bivariate multifractal formalism

The estimation of the multifractal spectrum (3) cannot be based on its formal definition but requires taking recourse to formulas that are numerically robust for discrete data, the so-called multifractal formalisms. The state-of-the-art multifractal formalism is constructed from the multiscale statistics of wavelet leaders [1], [2], has been first developed for multivariate data in [12], [13] and is briefly recalled in the following paragraphs.

Let ψ denote the mother wavelet, an oscillating reference pattern that is characterized by its number of vanishing moments N_ψ, a positive integer defined as $\psi \in C^{N_\psi - 1}$ and $\forall n = 0, \ldots, N_\psi - 1$, $\int_{\mathbb{R}} t^k \psi(t) dt \equiv 0$ and $\int_{\mathbb{R}} t^{N_\psi} \psi(t) dt \neq 0$ and that is designed such that the collection $\{\psi_{j,k}(t) = 2^{-j/2} \psi(2^{-j} t - k)\}_{(j,k) \in \mathbb{Z}^2}$ of its dilated and translated templates forms an orthonormal basis of $\mathcal{L}^2(\mathbb{R})$ [15]. The discrete wavelet transform coefficients $d_X(j,k)$ of X are defined as $d_X(j,k) = 2^{-j/2} \langle \psi_{j,k} | X \rangle$, where we have adhered to a L^1 normalization. Then, the *wavelet leaders* of X are defined as $\ell_X(j,k) \triangleq \sup_{\lambda' \subset 3\lambda_{j,k}} |d_X(\lambda')|$, where $\lambda_{j,k} = [k2^j, (k+1)2^j)$ denotes the dyadic interval of size 2^j and $3\lambda_{j,k}$ stands for the union of $\lambda_{j,k}$ with its 2 neighbors [1], [2]. It can be shown that wavelet leaders reproduce Hölder exponents in the limit of fine scales, $L_X(j,k) \sim C 2^{j h(t)}$ as $2^j \to 0$ for $t = 2^j k$. Consequently,

$$\frac{1}{n_j} \sum_{k=1}^{n_j} L_{X_1}(j,k)^{q_1} L_{X_2}(j,k)^{q_2} \sim c_q 2^{j \zeta(q_1, q_2)}, \; 2^j \to 0. \quad (4)$$

Most importantly, the so-called *scaling exponents* $\zeta(\mathbf{q})$ in (4) are tightly related to $\mathcal{D}(\mathbf{h})$ via their Legendre transform, the *bivariate Legendre spectrum*

$$\mathcal{L}(\mathbf{h}) = \inf_{\mathbf{q}} (1 + \langle \mathbf{q}, \mathbf{h} \rangle - \zeta(\mathbf{q})), \quad (5)$$

which provides an estimate for $\mathcal{D}(\mathbf{h})$ for large classes of processes, see [12].

C. Cumulant expansion of the bivariate Legendre spectrum

Using the arguments developed in [16], one can shown that for a large number of commonly used classes of multifractal processes with scaling exponents $\zeta(\mathbf{q})$, the cumulants $C_{p_1 p_2}(j)$ of the 2-variable vector of logarithm of leaders $(\ln L_{X_1}(j,k), \ln L_{X_2}(j,k))$ at scale 2^j take the form [13]

$$C_{p_1 p_2}(j) = c^0_{p_1 p_2} + j \, c_{p_1 p_2} \ln 2, \quad p_1 + p_2 \geq 1 \quad (6)$$

and the coefficients $c_{p_1 p_2}$ are related to the $\zeta(q_1, q_2)$ as

$$\zeta(q_1, q_2) = \sum_{p_1, p_2 \geq 0 :\; p_1 + p_2 \geq 1} c_{p_1 p_2} q_1^{p_1} q_2^{p_2} / (p_1! \; p_2!). \quad (7)$$

Further, from (6), estimators for $c_{p_1 p_2}$ can be defined as linear regressions of sample cumulants $\hat{C}_{p_1 p_2}(j)$:

$$\hat{c}_{p_1 p_2} \triangleq \sum_{j=j_1}^{j_2} w_j \hat{C}_{p_1 p_2}(j) / \ln 2, \quad (8)$$

over a range of scales $j \in (j_1, j_2)$, where w_j are linear regression weights.

By truncating the sum in (7) to the leading order terms $p_1, p_2 \geq 0 : \; 1 \leq p_1 + p_2 \leq 2$, we can gain insight into the information provided by the shape of the bivariate spectra $\mathcal{L}(\mathbf{h})$. The quadratic approximation $\zeta(q_1, q_2) \approx c_{10} q_1 + c_{01} q_2 + \frac{c_{20}}{2} q_1^2 + \frac{c_{02}}{2} q^2 + c_{11} q_1 q_2$ yields the expression

$$\mathcal{L}(h_1, h_2) \approx 1 + \frac{c_{02} b}{2} \left(\frac{h_1 - c_{10}}{b} \right)^2 + \frac{c_{20} b}{2} \left(\frac{h_2 - c_{01}}{b} \right)^2 - c_{11} b \left(\frac{h_1 - c_{10}}{b} \right) \left(\frac{h_2 - c_{01}}{b} \right), \quad (9)$$

where $b \triangleq c_{20} c_{02} - c_{11}^2 \geq 0$, showing that

- the position of the maximum of the bivariate spectrum is given by $\mathbf{h}^m = (c_{10}, c_{01})$
- c_{20} and c_{02} quantify the widths of the fluctuations independently for each component and
- c_{11} yields a leading order joint characterization of the regularity fluctuations of both components. As an extreme case, when $c_{11} = 0$, $\mathcal{L}(\mathbf{h}) = 1 + \frac{c_{20}}{2} \left(\frac{h_1 - c_{10}}{c_{20}} \right)^2 + \frac{c_{02}}{2} \left(\frac{h_2 - c_{01}}{c_{02}} \right)^2$ (i.e., it equals the sum of the univariate spectra up to a constant) and the regularity fluctuations of the components are independent (in consistency with the generic properties of multivariate $\mathcal{L}(\mathbf{h})$ proven in [12]).

D. Bivariate multifractal parameters in natural coordinates

Inspection of the expression (9) leads to conclude that the level sets and the support of $\mathcal{L}(\mathbf{h})$ are rotated and translated ellipses in the (h_1, h_2) plane. Therefore, the *natural* parameters for $\mathcal{L}(\mathbf{h})$ are given by its center $\mathbf{h}^m$, and by the rotation angle θ and the major and minor half-axes α_1 and α_2 of its support. Expressions for these quantities are obtained by straight-forward but tedious calculations, and are given by

$$\theta = \frac{1}{2} \arctan \Big(\frac{2 c_{11}}{c_{20} - c_{02}} \Big), \quad (10)$$

$$\alpha_1 = 2 \sqrt{\frac{c_{20} c_{02} - c_{11}^2}{-\sqrt{(c_{02} - c_{20})^2 + 4 c_{11}^2} - c_{02} - c_{20}}}, \quad (11)$$

$$\alpha_2 = 2 \sqrt{\frac{c_{20} c_{02} - c_{11}^2}{+\sqrt{(c_{02} - c_{20})^2 + 4 c_{11}^2} - c_{02} - c_{20}}}, \quad (12)$$

ISBN 978-90-827970-1-5

respectively. From these expressions, it can be seen that the linear eccentricity of the support

$$\epsilon \triangleq \sqrt{\alpha_1 - \alpha_2} = \frac{1}{2}\left(\sqrt{\gamma - c_{02} - c_{20}} - \sqrt{-\gamma - c_{02} - c_{20}}\right), \tag{13}$$

where $\gamma \triangleq \sqrt{(c_{02}-c_{20})^2 + 4c_{11}^2}$, increases with $|c_{11}|$, as expected. Moreover, in the special case $c_{02} = c_{20}$ (i.e., marginal spectra of equal width), $\theta = \pm 45°$, and $\alpha_{1,2} = 2\sqrt{-c_{20} \pm |c_{11}|}$; in other words, the spectrum remarkably flips between diagonal and anti-diagonal orientation as c_{11} changes sign. Finally, estimators $\hat{\theta}$, $\hat{\alpha}_1$, $\hat{\alpha}_2$ and $\hat{\epsilon}$ can be readily defined by replacing $c_{p_1p_2}$ with estimates (8) in (10-12).

III. Bivariate multifractal model process

A. Definition of bivariate multifractal random walk

Multifractal random walks (MRW) were originally proposed as realistic models for multifractal data [17]. Their construction is based on the increments of fractional Brownian motion (fBm), the reference Gaussian self-similar process [18], whose variance is modulated using an independent process whose properties mimic those of Mandelbrot cascades, and hence impart their multifractality to the MRW [4], [17]. Building on the unpublished work [14], a bivariate extension of MRW was proposed in [13], which we denoted bMRW and briefly summarize next.

The construction of bMRW requires two pairs of stochastic processes: First, a pair of increments of fBm, $\big(G_1(t), G_2(t)\big)$, which is determined by two self-similarity parameters, H_1 and H_2, and a point covariance Σ_{ss}. Its correlation coefficient is hereafter referred to as ρ_{ss}. These processes can be constructed as a specific case of the operator fractional Brownian motion framework developed in [19]. Second, a pair of Gaussian processes $\big(\omega_1(t), \omega_2(t)\big)$ with prescribed covariance function Σ_{mf}, with entries given by

$$\{\Sigma_{mf}\}_{ij}(k,l) = \rho_{mf}(i,j)\lambda_i\lambda_j \log\left(\frac{T}{|k-l|+1}\right), \; i = 1,2 \tag{14}$$

for $|k-l| \leq T-1$ and 0 otherwise, where T is an arbitrary integral scale. To simplify notations, we consider $\rho_{mf}(1,1) = \rho_{mf}(2,2) = 1$, and $\rho_{mf}(1,2) = \rho_{mf}$. Both pairs of processes are numerically synthesized as described in [20].

Finally, each component $i = 1, 2$ of bMRW is defined as

$$X_i(t) = \sum_{k=1}^{t} G_i(k) e^{\omega_i(k)}. \tag{15}$$

B. Multifractal properties

As detailed in [13], following [14], [17], the bivariate scaling exponents of bMRW are conjectured to take the form (7), with and $c_{10} = H_1 + \lambda_1^2/2$, $c_{01} = H_2 + \lambda_2^2/2$, $c_{20} = -\lambda_1^2$, $c_{02} = -\lambda_2^2$, and $c_{11} = -\rho_{mf}\lambda_1\lambda_2$. Moreover, $c_{p_1p_2} \equiv 0$, $\forall (p_1, p_2)$ such that $p_1 + p_2 \geq 3$; therefore, the second order approximation developed in Section II-C (in particular, (9)) is exact for bMRW.

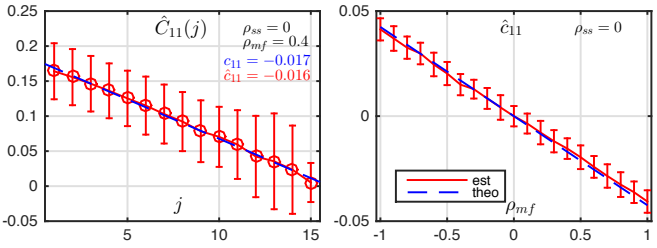

Fig. 1. **Log-scale diagram $\hat{C}_{11}(j)$** and estimation performance for c_{11} (from left to right).

C. Correlation and dependence

The dependence between the components of bMRW is clearly controlled by the correlation parameters ρ_{ss} and ρ_{mf} of the self-similar random walk and multifractal cascade components entering its construction, respectively; we therefore identify here expressions for these parameters involving quantities that can be readily measured from data. An estimator for ρ_{mf} can be defined as [13]

$$\hat{\rho}_{mf} \triangleq -\hat{c}_{11}/\sqrt{|\hat{c}_{20}\hat{c}_{02}|}. \tag{16}$$

To identify the parameter ρ_{ss}, we first derive the expression for the Pearson correlation ρ_{bMRW} of the increments of the components of bMRW. The increments are, for each k, the product of mutually independent Gaussian and log-normal random variables, see (15); using elementary expressions for the product, expectation and variance of log-normal random variables, we therefore have

$$\begin{aligned}
\mathbb{E}[\Delta X_i(k)] &= \mathbb{E}[G_i(k)] \cdot \mathbb{E}[e^{\omega_i(k)}] = 0 \\
\mathrm{Var}[\Delta X_i(k)] &= \sigma_i^2 (e^{\lambda_i^2 \log(T)} - 1) e^{\lambda_i^2 \log(T)} \\
&\quad + \sigma_i^2 e^{\lambda_i^2 \log(T)} = \sigma_i^2 e^{2\lambda_i^2 \log(T)} \\
\mathbb{E}[\Delta X_1(k) \Delta X_2(k)] &= \mathbb{E}[G_1(k)G_2(k)] \cdot \mathbb{E}[e^{\omega_1(k)+\omega_2(k)}] \\
&= \rho_{ss}\sigma_1\sigma_2 e^{\frac{1}{2}(\lambda_1^2+\lambda_2^2+2\rho_{mf}\lambda_1\lambda_2)\log(T)},
\end{aligned}$$

and thus

$$\begin{aligned}
\rho_{bMRW} &= \frac{\mathbb{E}[\Delta X_1(k)\Delta X_2(k)] - \mathbb{E}[\Delta X_1(k)]\mathbb{E}[\Delta X_2(k)]}{\sqrt{\mathrm{Var}[\Delta X_1(k)]\mathrm{Var}[\Delta X_2(k)]}} \\
&= \frac{\rho_{ss}\sigma_1\sigma_2 e^{\frac{1}{2}(\lambda_1^2+\lambda_2^2+2\rho_{mf}\lambda_1\lambda_2)\log(T)}}{\sigma_1\sigma_2 e^{(\lambda_1^2+\lambda_2^2)\log(T)}} \\
&= \rho_{ss} e^{\left(\rho_{mf}\lambda_1\lambda_2 - \frac{1}{2}(\lambda_1^2+\lambda_2^2)\right)\log(T)}.
\end{aligned} \tag{17}$$

Consequently, $\rho_{bMRW} = \rho_{ss} \cdot f(\rho_{mf}, \lambda_1, \lambda_2)$ takes the form of a product of the correlation coefficient ρ_{ss} of the random walk components $G_i(k)$ and a nonlinear function in the parameters of the multifractal components $e^{\omega_i(k)}$. Notably, this implies that the Pearson correlation coefficient can equal zero (in case $\rho_{ss} = 0$) even when the data are actually highly dependent ($\rho_{mf} \neq 0$). Thus, the bivariate multifractal spectrum can be seen as capturing transient local dependencies beyond second order correlations, see [13] and Section IV.

Further, in view of the model described in Section III, the parameters ρ_{ss} and ρ_{mf} constitute natural expansion

ISBN 978-90-827970-1-5 © EURASIP 2018

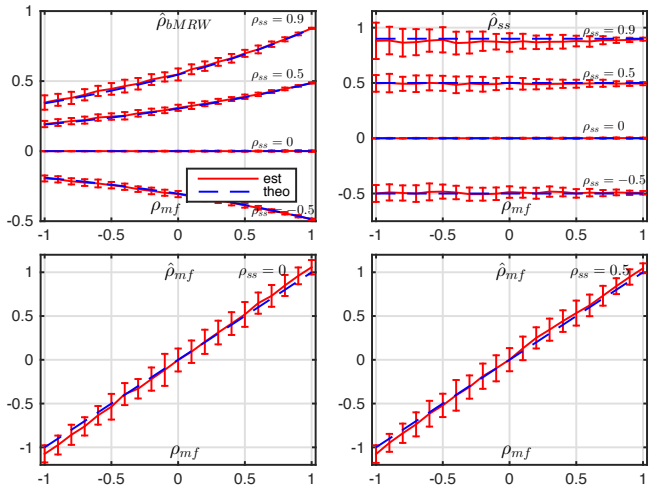

Fig. 2. **Model and estimation for dependence parameters.** Pearson correlation coefficient ρ_{bMRW} (top left), self-similar random walk correlation ρ_{ss} (top right), and multifractal correlation ρ_{mf} (bottom row), for several ρ_{ss}.

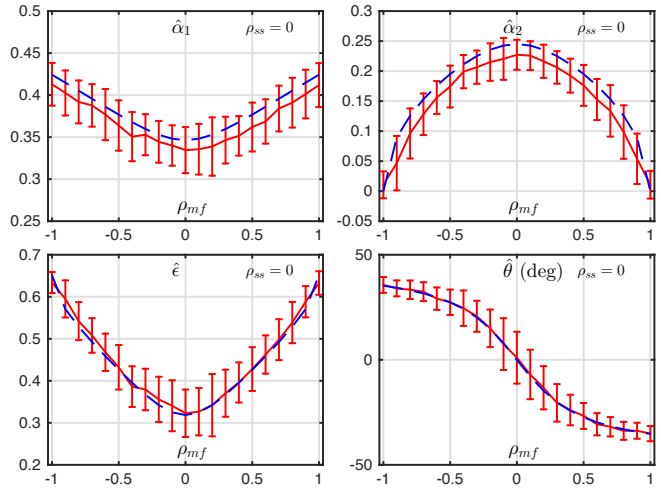

Fig. 3. **Model and estimation for natural bivariate multifractal parameters.** Semi-axes α_1 (top left) and α_2 (top right), eccentricity ϵ (bottom left) and orientation θ (bottom right).

coefficients for the joint dependence of X. Upon substitution of $c_{11} = -\rho_{mf}\lambda_1\lambda_2$, $c_{20} = -\lambda_1^2$, $c_{02} = -\lambda_2^2$, we can define a natural estimator for ρ_{ss} as

$$\hat{\rho}_{ss} \triangleq \hat{\rho}_{bMRW} e^{\left(\hat{c}_{11} - \frac{1}{2}(\hat{c}_{20}+\hat{c}_{02})\right)\log(T)}. \tag{18}$$

IV. Estimation performance assessment

A. Monte Carlo simulations and parameter setting

Estimation performance is analyzed through Monte Carlo simulations over 100 independent copies of bMRW of sample size $n = 2^{18}$. The parameters of the process are set to $(H_1, H_2) = (0.65, 0.75)$, $(\lambda_1, \lambda_2) = (\sqrt{0.03}, \sqrt{0.06})$, and several values for ρ_{ss} and ρ_{mf} are considered. The integral scale in (14) is set to $T = n$. Wavelet analysis is conducted with a Daubechies least asymmetric wavelet, with $N_\psi = 3$.

B. Bivariate multifractality parameter c_{11}

The estimation performance for univariate parameters c_{10}, c_{01}, c_{20}, and c_{02} remains unaltered in the multivariate setting, and has been documented elsewhere (see, e.g., [2]). Here we focus on the multivariate parameter c_{11}. Fig. 1 (left) shows that estimates of the quantities $C_{11}(j)$ behave as a clean, linear function of octaves j as postulated by (6), allowing the estimation of parameter $\hat{c}_{11}$ by linear regression. Further, Fig. 1 (right) clearly indicates the excellent performance of the estimates $\hat{c}_{11}$ for all values of ρ_{mf}, with negligible bias and variance independent of ρ_{mf}.

C. Correlation and dependence

Figure 1 (top left) shows that the Pearson correlation ρ_{bMRW} is a nonlinear function of the multifractal correlation ρ_{mf} and tightly follows the predicted values (17). Moreover, and notably, $\rho_{bMRW} = 0$ when ρ_{ss} even if $\rho_{mf} \neq 0$, illustrating that ρ_{mf} measures a type of dependence to which the second-order Pearson correlation is totally blind. Further, Fig. 2 (top right) shows that estimates $\hat{\rho}_{ss}$ remain constant with ρ_{mf}, and precisely recover the true values, with negligible bias. Interestingly, the variances of $\hat{\rho}_{ss}$ and $\hat{\rho}_{bMRW}$ decrease with increasing ρ_{mf} and decreasing ρ_{ss}; a precise modeling of this phenomenon is left for future work. Finally, Fig. 2 (bottom row) shows estimation performance of $\hat{\rho}_{mf}$, already reported in [13]. Here, the performance is moreover shown to be independent of ρ_{ss}; further, the results indicate that it is largely unaffected by the true value of ρ_{mf}.

D. Second order multifractal analysis in natural coordinates

Fig. 3 illustrates the estimation performance for the natural parameters θ, $\alpha_{1,2}$ and ϵ, defined in (10-13), for the quadratic bivariate multifractal model. It shows that the estimates for θ, $\alpha_{1,2}$ and ϵ overall closely reproduce the theoretical values. In particular, estimates for the rotation angle θ (i.e., the orientation of the multifractal spectra in the (h_1, h_2) plane) are found to be highly accurate. The estimates for both the minor and major half-axes, α_1, α_2 are affected by a slight but systematic negative bias, for all ρ_{mf}. However, this bias has no negative effect on the estimates for the linear eccentricity ϵ, which are very satisfactory. Similar results are obtained for other values of ρ_{ss} and not shown for space reasons (here, ρ_{ss}). Overall, this leads to conclude that while the scale of the quadratic multifractal model is slightly underestimated, estimates for its shape and orientation are highly accurate.

This is further investigated in Fig. 4, which illustrates the level sets of the Legendre spectrum $\mathcal{L}$ (middle row) and its estimate $\hat{\mathcal{L}}$ (bottom row), for $\rho_{ss} = 0$ and several values of ρ_{mf}, together with the major and minor half axes of the second order model (blue dashed lines) and their estimates (red lines). The results reveal an excellent agreement between the estimates and their true values in all cases. Moreover, they indicate that, despite the slight negative bias of $\hat{\alpha}_1$ and $\hat{\alpha}_2$, these natural parameters of the second order model provide on

ISBN 978-90-827970-1-5 © EURASIP 2018

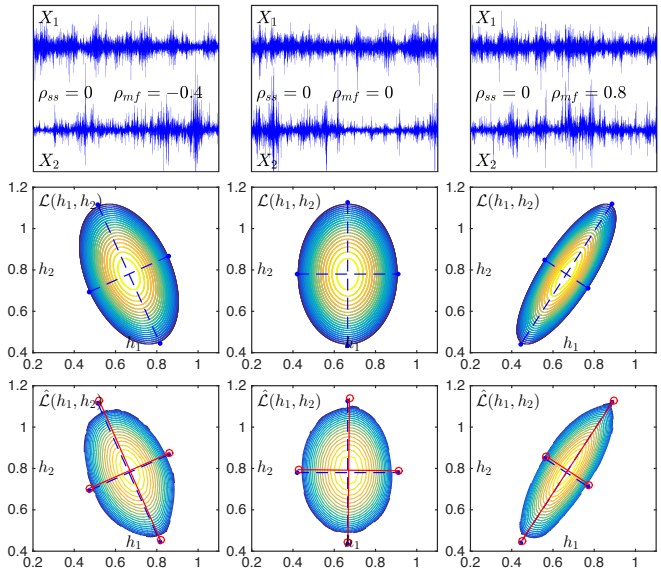

Fig. 4. **Legendre spectra.** Sample paths (top row), true Legendre spectra $\mathcal{L}$ (middle row) and estimates $\hat{\mathcal{L}}$ (bottom row), for three bMRW with $\rho_{ss} = 0$ and $\rho_{mf} = -0.4$ (left column), $\rho_{mf} = 0$ (middle column), and $\rho_{mf} = 0.8$ (right column). The true and estimated minor and major axes are shown in blue-dashed and red-solid lines, respectively.

average more accurate estimates of the size of the support of the multifractal spectrum (hence, the domain of joint regularity fluctuations) than the unconstrained Legendre spectra $\mathcal{L}$, which are further shrank as compared to theory.

It is worth pointing out that for all the examples considered in Fig. 4 (top row), $\rho_{ss} = 0$. Thus, $\rho_{bMRW} = 0$ and Pearson correlation is unable to distinguish those time series. However, their multifractal spectra $\mathcal{L}$ clearly capture a form of higher-order statistical dependence beyond Pearson correlation, and fully characterize these processes (see also [13]). This information is conveniently summarized in the *natural* parameters θ and $\alpha_{1,2}$, which characterize the orientation and strength of joint regularity fluctuations.

V. Conclusion

In this work, the identification and estimation of second-order joint multifractal properties for bivariate processes was considered. Expressions for second order parameters in natural coordinates were derived, and shown to provide an intuitive and versatile description for the higher-order dependencies of the data. Crucially, these parameters distinguish dependencies that the usual Person correlation cannot identify. Moreover, an expression for the joint dependence structure was provided, enabling a factorization into an (additive) self-similar random-walk correlation and a (multiplicative) multifractal correlation. Estimators for the associated (multifractal and correlation) parameters have been defined, and their performance was assessed on synthetic data and shown to be highly satisfactory. These developments open new and promising perspectives for the analysis of real-world multivariate data, including applications in neuroscience, which are currently being explored.

Acknowledgment

Work supported by ANR-16-CE33-0020 MultiFracs, France.

References

[1] S. Jaffard, "Wavelet techniques in multifractal analysis," in *Fractal Geometry and Applications: A Jubilee of Benoît Mandelbrot, M. Lapidus and M. van Frankenhuijsen, Eds., Proc. Symposia in Pure Mathematics*, vol. 72(2). AMS, 2004, pp. 91–152.

[2] H. Wendt, P. Abry, and S. Jaffard, "Bootstrap for empirical multifractal analysis," *IEEE Signal Proc. Mag.*, vol. 24, no. 4, pp. 38–48, 2007.

[3] K. Kiyono, Z. R. Struzik, N. Aoyagi, and Y. Yamamoto, "Multiscale probability density function analysis: non-Gaussian and scale-invariant fluctuations of healthy human heart rate," *IEEE Trans. Biomed. Eng.*, vol. 53, no. 1, pp. 95–102, Jan. 2006.

[4] B. B. Mandelbrot, "Intermittent turbulence in self-similar cascades: divergence of high moments and dimension of the carrier," *J. Fluid Mech.*, vol. 62, pp. 331–358, 1974.

[5] P. Ciuciu, G. Varoquaux, P. Abry, S. Sadaghiani, and A. Kleinschmidt, "Scale-free and multifractal time dynamics of fMRI signals during rest and task," *Front. Physiol.*, vol. 3, Jun. 2012.

[6] M. Doret, H. Helgason, P. Abry, P. Gonçalvès, C. Gharib, and P. Gaucherand, "Multifractal analysis of fetal heart rate variability in fetuses with and without severe acidosis during labor," *Am. J. Perinatol.*, vol. 28, no. 4, pp. 259–266, 2011.

[7] R. Fontugne, P. Abry, K. Fukuda, D. Veitch, K. Cho, P. Borgnat, and H. Wendt, "Scaling in internet traffic: a 14 year and 3 day longitudinal study, with multiscale analyses and random projections," *IEEE/ACM T. Networking*, vol. 25, no. 4, 2017.

[8] A. Johansen and D. Sornette, "Finite-time singularity in the dynamics of the world population, economic and financial indices," *Physica A*, vol. 294, pp. 465–502, 2001.

[9] C. Meneveau, K. Sreenivasan, P. Kailasnath, and M. Fan, "Joint multifractal measures - theory and applications to turbulence," *Phys. Rev. A*, vol. 41, no. 2, pp. 894–913, 1990.

[10] T. Lux, "Higher dimensional multifractal processes: A GMM approach," *Journal of Business and Economic Statistics*, vol. 26, pp. 194–210, 2007.

[11] S. Jaffard, P. Abry, and H. Wendt, *Irregularities and Scaling in Signal and Image Processing: Multifractal Analysis*. Singapore: World scientific publishing, 2015, pp. 31–116.

[12] S. Jaffard, S. Seuret, H. Wendt, R. Leonarduzzi, S. Roux, and P. Abry, "Multivariate multifractal analysis," *Appl. Comp. Harm. Anal.*, 2018, in press.

[13] H. Wendt, R. Leonarduzzi, P. Abry, S. Roux, S. Jaffard, and S. Seuret, "Assessing cross-dependencies using bivariate multifractal analysis," in *IEEE Int. Conf. Acoust., Speech, and Signal Proces. (ICASSP)*, Calgary, Canada, April 2018.

[14] E. Bacry, J. Delour, and J. F. Muzy, "A multivariate multifractal model for return fluctuations," *arXiv preprint cond-mat/0009260*, 2000.

[15] S. Mallat, *A Wavelet Tour of Signal Processing*. San Diego, CA: Academic Press, 1998.

[16] B. Castaing, Y. Gagne, and M. Marchand, "Log-similarity for turbulent flows," *Physica D*, vol. 68, no. 3-4, pp. 387–400, 1993.

[17] E. Bacry, J. Delour, and J.-F. Muzy, "Multifractal random walk," *Phys. Rev. E*, vol. 64: 026103, 2001.

[18] G. Samorodnitsky and M. Taqqu, *Stable non-Gaussian random processes*. New York: Chapman and Hall, 1994.

[19] G. Didier and V. Pipiras, "Integral representations and properties of operator fractional Brownian motions," *Bernoulli*, vol. 17, no. 1, pp. 1–33, 2011.

[20] H. Helgason, V. Pipiras, and P. Abry, "Fast and exact synthesis of stationary multivariate Gaussian time series using circulant embedding," *Signal Proc.*, vol. 91, no. 5, pp. 1123–1133, 2011.